Pergamon

Phys. Chem. Earth (A), Vol. 26, No. 3, pp. 165–171, 2001

1464-1895/01/$ - see front matter

PII: S1464-1895(01)00041-2

Study of External Path Delay Correction Techniques for High Accuracy Height Determination with GPS

O. Bock[1,2], J. Tarniewicz[2], C. Thom[2], J. Pelon[3] and M. Kasser[4]

[1]Ecole Supérieure des Géomètres et Topographes / CNAM, 72000 LeMans, France
[2]Laboratoire d'Optoélectronique et Microinformatique / IGN, 94165 Saint-Mandé Cedex, France
[3]Service d'Aéronomie / CNRS, Université Pierre et Marie Curie, 75252 Paris Cedex 05, France
[4]Laboratoire de Recherche en Géodésie / IGN, 94165 Saint-Mandé Cedex, France

Received 4 August 2000; accepted 11 December 2000

Abstract. For specific applications such as permanent GPS network calibration and national leveling network surveying, a vertical accuracy of ~1 mm for observing durations of a few hours to a few days at maximum in 10–100-km baselines would be required. To achieve a 1-mm accuracy in height determinations with differential-GPS measurements, path delay must be corrected with an accuracy of ~0.3 mm. This level of accuracy is not achievable with standard GPS data analysis procedures. External correction from a water vapor remote sensing technique is therefore necessary. Microwave radiometers, which have been most extensively used for this purpose, solar spectrometers, DIAL and Raman lidars are considered in this paper. The principle and performance of these techniques is reviewed in the context of wet path delay retrieving. Namely, we evaluate the errors arising during the conversion of raw measurements to wet path delay, using retrieval coefficients or standard profiles. It is shown that changes in temperature profiles can produce errors of up to 1 cm in wet path delay with microwave radiometers. Similarly, mismodeled temperature profiles can produce errors of 2-3 mm in wet path delay with DIAL and Raman lidars. Raman lidar offers the possibility to retrieve the temperature profile from total air density. Assuming that absolute concentrations of water vapor and dry gases can be retrieved, the accuracy would be unbiased. In addition, Raman lidar would also allow for the correction of hydrostatic path delay without requiring the use of mapping functions. This might reduce the residual errors due to horizontal pressure and temperature gradients. This technique will therefore be investigated in more details in a future study.

Correspondence to : O. Bock

1 Introduction

The Global Positioning System (GPS) has been extensively used in the last decade for many geodetic applications (crustal dynamical processes, absolute see level change, natural hazards). With the present state of the art in GPS data analysis, the accuracy is about 1–2 mm in horizontal coordinates and 5–10 mm in the vertical coordinate, for baselines ranging from a few km to 1000 km. Observing durations are of a few days, for typical measurement campaigns, or continuous for the monitoring of slow processes such as crustal dynamics.

The main error source in height determination with dual-frequency GPS is path delay in the troposphere, especially due to the inhomogeneity and variability of water vapor. A 1-mm error in zenith tropospheric delay (ZTD) can produce biases in station height of 2–6 mm, for elevation cutoff angles between 5 and 25° (Santerre, 1991). Two strategies are commonly used for tropospheric path delay correction in GPS data analysis: parameter estimation and external correction. In the former, path delay is modeled and parameters are estimated from GPS measurements (Tralli and Lichten, 1990). In the latter, path delay is measured by a remote sensing technique, usually water vapor radiometry, and path delay corrections are applied to GPS signals during the analysis (Ware, 1993). Both strategies have led to similar accuracies in most applications involving medium (100 km) to long (1000 km) baselines, and observing durations between days and years (Dodson et al., 1996; Johansson et al., 1998).

The Institut Géographique National (IGN) is involved with more specific applications such as permanent GPS network calibration and national leveling network surveying. There, an accuracy in the vertical of ~1 mm, for observing durations of a few hours in 10–100-km baselines would be required. Accurate height determination from sub-daily sessions has several limitations not encountered in long sessions. Among these are the variations in the satellite constellation (Santerre, 1991) and, most limiting, the

particular atmospheric conditions that may exist during data acquisition.

To achieve an accuracy in relative height determination with GPS at the 1-mm level, ZTD should be corrected with an accuracy better than ~0.3 mm. Unfortunately, this level of accuracy is not achievable with the present GPS data analysis strategies. Even in the future, parameter estimation is unlikely to achieve this level of accuracy due to the strong correlation between vertical coordinates and estimated zenith path delay parameters. Additionally, this strategy uses mapping functions, which usually have been derived from standard atmospheric models or radiosonde profiles (Niell, 1996). Mapping functions might be useful for long term geodetic analyses (of order years), where accidental meteorological events can be smoothed out. For short observing sessions, specific atmospheric conditions can be responsible for significant variations in wet path delay. Errors in zenith wet delay (ZWD) of up to 5–8 cm have been observed during the passage of weather fronts (Elgered, 1993; Ichikawa et al., 1995). Such phenomena are most probably responsible for the observed day-to-day variations in station height, amounting commonly to a few centimeters (Johansson et al., 1998). Hence, external correction for path delay is the preferred strategy, in this context.

Recent results, using water vapor radiometers, have shown accuracies in the vertical between 1 and 3 mm (Ware et al., 1993; Glaus et al., 1995; Alber et al., 1997). These are very encouraging, but need further demonstration of their capability to achieve such accuracies in most atmospheric conditions. Especially, microwave radiometers measure an integrated water vapor content, which might lead to biases in wet path delays, in strongly layered atmospheres. In addition, hydrostatic path delay cannot be inferred from common dual channel radiometers. It is usually corrected from surface pressure and a mapping function. Horizontal gradients in the hydrostatic path delay are commonly associated with weather fronts. In such cases, mapping functions might produce errors in path delay up to a few cm (Ichikawa et al., 1995; MacMillan and Ma, 1998). Moreover, rolls and thermals in the atmospheric boundary layer have been predicted to produce errors of up to 2-cm in station heights (Bock et al., 2000). Weather fronts and boundary layer inhomogenities are the most important processes to be resolved for short term GPS observation in medium range networks.

In the present paper, we first review the principle and performance of different water vapor remote sensing techniques presently available. Then we focus on the necessity for making spatially resolved measurements (achieved with lidars, for example) compared to integrated measurements (achieved with microwave radiometers or solar hygrometers). Finally, we discuss more precisely the potential of the Raman lidar technique, which might retrieve both wet and hydrostatic path delays from density profiles.

2 Water vapor sensing techniques

In this section we will derive the relationship between the physical variables sensed by the different techniques and wet path delay, defined by :

$$\Delta L_w = k \int \frac{\rho_v(s)}{T(s)} ds \tag{1}$$

with $k = 1.723\,\mathrm{K/(kg/m^3)}$, $\rho_v(s)$ the water vapor density ($\mathrm{kg/m^3}$) and $T(s)$ the atmospheric temperature (K). Note that this definition for wet path delay is sufficient for evaluation of errors from the different sensing techniques. However, for an accurate path delay correction a more complete definition for wet path delay should be used (see. e.g., Elgered, 1993).

2.1 Water vapor radiometers

Microwave radiometers, usually referred to as water vapor radiometers (WVRs), have been most widely used for external path delay correction in GPS and Very Long Baseline Interferometry (VLBI) data analysis. Ground-based WVRs measure sky brightness temperatures expressed by (Elgered, 1993):

$$T_{b,\nu} = T_{bo,\nu} e^{-\tau(\nu,\infty)} + \int_0^\infty T(s)\alpha(\nu,s) e^{-\tau(\nu,s)} ds \tag{2}$$

where ν is the frequency, $T_{bo,\nu}$ the cosmic background temperature (~2.8 K), $\alpha(\nu,s)$ the total attenuation coefficient, due to water vapor, oxygen and liquid water, and $\tau(\nu,s) = \int_0^s \alpha(\nu,s')ds'$ is the opacity. At high opacities, e.g., at low elevation angles, $T_{b,\nu}$ becomes insensitive to water vapor. This is a saturation problem, which is overcome when using either linearized brightness temperatures or opacities as observables (Elgered, 1993). The effect of oxygen attenuation is modeled from standard atmospheres with sufficient accuracy. Attenuation due to liquid water, on the other hand, must be sensed by the radiometer, because of its unpredictable content in the atmosphere. Therefore, measurements are made on two frequencies, allowing either for the estimation or elimination (by combination of the observed brightness temperatures) of the liquid water effect. In the case of linearized brightness temperatures, the liquid water independent observable writes then (Wu, 1978):

$$\begin{aligned} X_{WVR} &= \int_0^\infty \left[T(s) - T_{bo,\nu_1}\right] \left[\frac{\alpha_v(\nu_1,s)}{\nu_1^2} - \frac{\alpha_v(\nu_2,s)}{\nu_2^2}\right] ds \\ &\equiv \int_0^\infty W'(s) \frac{\rho_v(s)}{T(s)} ds \end{aligned} \tag{3}$$

where $W'(s)$ is a weighting function, which can be identified from the above equality, the prime indicating that the observable is obtained from linearized brightness temperatures. The water vapor attenuation coefficient $\alpha_v(v,s)$ appearing in Eq.(3) is proportional to the concentration of water vapor molecules. However, it is also sensitive to temperature and atmospheric pressure (Rosenkranz, 1993). In addition, temperature appears also explicitly in the first integral. Assuming a constant $W'(s)=W'_m$ is a fundamental source of bias. It can, however, be minimized by choosing an appropriate couple of frequencies (Wu, 1978) and possibly by parameterizing W'_m with surface temperature.

Another fundamental source of bias stems from the linearization of brightness temperatures, namely with the introduction of an effective temperature (Elgered, 1993). This is usually done to remove the explicit temperature dependence (first square brackets) in Eq.(3). The error associated with this assumption is smaller than with $W'(s)=W'_m$ and will therefore be neglected in the following.

Instrumental sources of biases are mainly related to the calibration of WVRs. The most common technique (known as "tip-curve" calibration) consists in performing sky brightness measurements at different zenith angles. This allows, using a mapping function, to adjust offset and gain parameters for the instrument (Elgered, 1993). However, this approach is limited by atmospheric inhomogeneity, where mapping functions are in error, and by liquid water present in clouds and rainfall. For drops larger than a few tenths of mm, ZWD might be overestimated by a few cm (Elgered, 1993).

The theoretical precision in ZWD estimates has been evaluated to be at the 2-mm level, RMS, for long observing periods (England et al., 1992; Elgered, 1993). Instrumental accuracy has been evaluated by comparing different WVRs. Biases in ZWD between 1–3 cm have been reported, while the standard deviation in estimates was about 3–5 mm for the different instruments (Rocken et al., 1991). This shows that calibration errors are dominating in these instruments. A better parameterization of retrieval coefficients and instrumental factors with surface temperature might possibly improve the accuracy. Comparisons with radiosonde measurements showed biases of 1–2 cm (Elgered, 1993). However, it is well recognized that in situ sensors mounted on radiosondes have a dry bias at relative humidities below 10–20 % (Westwater et al., 1989). More recent techniques, such Raman lidars and IR spectrometers have shown ZWD retrieval accuracy with WVRs at the 5-mm level (England et al., 1992; Sierk et al., 1997).

2.2 Infrared solar hygrometers and spectrometers

These are ground-based instruments measuring the solar radiance having traversed the atmosphere, in the near IR spectral band containing absorption lines of water vapor. The signal measured by either an infrared solar hygrometer (IRSH) or an infrared solar spectrometer (IRSS) at wavelength λ can be written:

$$S_\lambda = k_\lambda F_{0\lambda} e^{-\tau(\lambda)} \tag{4}$$

where k_λ is a system spectral sensitivity factor, including detector quantum efficiency and filter transmittance, $F_{0\lambda}$ is the outer atmosphere solar spectral irradiance, and $\tau(\lambda)=\int_0^\infty \alpha(\lambda,s')ds'$ is the optical depth. The attenuation coefficient $\alpha(\lambda,s')$ is composed of Rayleigh scattering by atmospheric gases, Mie scattering by aerosols, and absorption by water vapor. For an IRSS, S_λ is readily measured as a function of λ, while for an IRSH it is integrated over the filter bandpass.

Wet path delay might be estimated by infrared techniques in a very similar manner as with WVR. Optical depth might be considered as the observable:

$$X_{IR} = \int_0^\infty \alpha_v(\lambda,s)ds \equiv \int_0^\infty G(s)\frac{\rho_v(s)}{T(s)}ds \tag{5}$$

and the weighting function $G(s)\approx G_m$ would be taken as a constant. One can therefore expect similar performance for both microwave and infrared radiometers.

In IRSHs the ratio between two spectrally integrated radiances, one over a water vapor absorption band, and another in a nearby transmission window is performed (Reagan et al., 1992). This is a differential absorption approach. There, absorption band models are required to relate the spectrally integrated optical depth to the integrated precipitable water vapor (or PW for short). This relationship is a major source of uncertainty in PW retrievals from IRSHs (Sierk et al., 1997). In addition, since the two measured bands are spectrally separated, scattering by aerosols becomes a limiting factor. The accuracy of IRSHs is typically at the 10% level in PW, i.e., between 5–20 mm in wet path delay, for typical values of PW in the range 10–30 mm.

On the other hand, IRSSs are capable of resolving individual water vapor rotational absorption lines. This avoids the use of absorption band models. The approach followed by Sierk et al., 1997, is to resolve water vapor spectral lines in the vicinity of 925 nm. The PW is estimated by fitting the optical depth due to water vapor absorption to a high resolution spectral model assuming standard temperature and pressure profiles to account for line broadening. PW is modeled from a two-piece linear function in relative humidity where the surface value is measured and the value at the connection point between the two layers is also fitted by the algorithm. The sensitivity factor k_λ, as a function of λ, is calibrated with the help of an external light source. This instrument has demonstrated a standard deviation of 0.75 mm in PW, or 4.8 mm in wet

path delay. This level of accuracy is comparable to that achieved with WVRs. However, these authors state that the main limiting factor is the model for spectral lines (2–5 %), while calibration errors are below 1 %. This is in contrast with WVRs where calibration errors are dominating.

2.3 Lidars

Two lidar techniques are used by meteorologists for sensing water vapor: differential absorption (DIAL) and Raman scattering. DIAL lidars use narrow band tunable lasers, transmitting a short light pulse into the atmosphere at two wavelengths: one centered on an absorption line of water vapor, and the other out of the line (Wulfmeyer and Bösenberg., 1998). The transmitted light is backscattered by atmospheric gases and aerosols and is detected with a telescope, spectral filters and photomultiplier tubes. A photon counting system allows for the integration of temporal slices of the backscattered light over several laser shots. The raw measurement thus is a slant profile of photon counts. The ratio of the photon counts at the two wavelengths allows for the determination of the water vapor concentration. The conversion to wet path delay would then be achieved after water vapor is integrated according to Eq.(1), which requires a temperature profile.

The principle of Raman lidar is quite similar, except that a single wavelength is transmitted, which needs not be finely tuned (Whiteman et al., 1992). This is a major difference between the two techniques and makes Raman lidars more attractive for transportable systems like WVRs. However, Raman scattering is a very weak optical process and requires either a relatively high optical power and large telescope or averaging times of order minutes. Despite these restrictions, we shall consider in more details the performance of Raman lidars and believe they might be compatible with the goal of external path delay correction for GPS.

In most Raman lidars, at least three receiving channels are implemented for the detection of elastic and inelastic backscattered light. The measured signal (photon counts), for a single laser shot, can be written as follows (Goldsmith et al., 1998):

$$S_x(z) = k_x \frac{A_r}{z^2} O(z) T_{\lambda_0}(z) T_{\lambda_x}(z) \sigma_{\lambda_x} N_x(z) \Delta z \qquad (6)$$

where 'x' denotes the channel (either water vapor, nitrogen, or elastic backscatter), k_x is an instrumental calibration parameter, including the number of photons transmitted by laser shot, the optical losses of the system and the quantum efficiency of the detector, A_r is the receiver (telescope) area, $O(z)$ is the overlap function assumed in the following to be $O(z)=1$, $T_{\lambda_0}(z)$ and $T_{\lambda_x}(z)$ are atmospheric transmissions between the ground and range z, where λ_0 denotes the laser wavelength and λ_x the backscattered radiation wavelength, σ_{λ_x} and $N_x(z)$ are the cross-section and concentration of the molecule responsible for the backscatter at the Raman shifted wavelength λ_x, respectively, and Δz is the spatial resolution of the lidar (usually determined by the counting rate). For the case of aerosols, the product $\sigma_{\lambda_x} N_x(z)$ is replaced by the extinction coefficient β_{λ_0}. The signal equation for a DIAL lidar is quite similar to Eq.(6). However, it would not allow for the retrieval of $\rho_d(z)$. In both lidar techniques, a pressure and temperature dependence of σ_{λ_x} with altitude might be included from a radiosounding.

Assuming an absolute calibration of the instrument is performed, such that water vapor and dry air densities can be retrieved from water vapor and nitrogen channels:

$$\rho_v(z) = \frac{M_v}{N_A} N_{WV}(z) \qquad (7)$$

$$\rho_d(z) = M_d \frac{N_d}{N_{N_2}} N_{N_2}(z) \qquad (8)$$

where M_v and M_d refer to the molecular weights of water vapor and dry air, respectively, and the ratio $N_{N_2} / N_d \approx 0.78$ is the molar fraction of nitrogen, and N_A is Avogadro's number (Salby, 1996). From the signal Eq.(6), it is evident that transmission needs be modeled at wavelengths λ_0, λ_{WV} and λ_{N_2}. For $\lambda_0 = 355$ nm, these wavelengths are $\lambda_{WV} = 408$ nm and $\lambda_{N_2} = 387$ nm. The difference in transmissions between such separated wavelengths might be significant, due to Rayleigh scattering by atmospheric gases and Mie scattering by aerosols. While Rayleigh scattering is sufficiently well modeled from standard atmospheres or radiosonde data, aerosol extinction must be calibrated from the elastic backscatter signal (Whiteman et al., 1992).

Instrumental parameters, k_x, are commonly calibrated with respect to radiosondes, WVRs or GPS derived PW (Goldsmith et al., 1998). It is evident that with such a calibration, the accuracy of lidar derived water vapor profiles will be on the level of the above-mentioned techniques. Independent calibration methods are thus required, which do not rely on external sounding techniques. This is a second approach, which requires proper calibration of all the elements in the instrument, especially filter spectral transmission and detector quantum efficiency (Sherlock et al., 1999). In addition, uncertainties in Raman cross section models will then be a limiting factor.

Raman lidars perform well at night-time, with a precision between 2 and 5 % in mixing ratio (ρ_v / ρ_d), i.e., 0.4–1 mm in wet path delay, for profiles up to 6–7 km (Whiteman et al., 1992). However, at daytime background noise becomes the predominant error source. Two

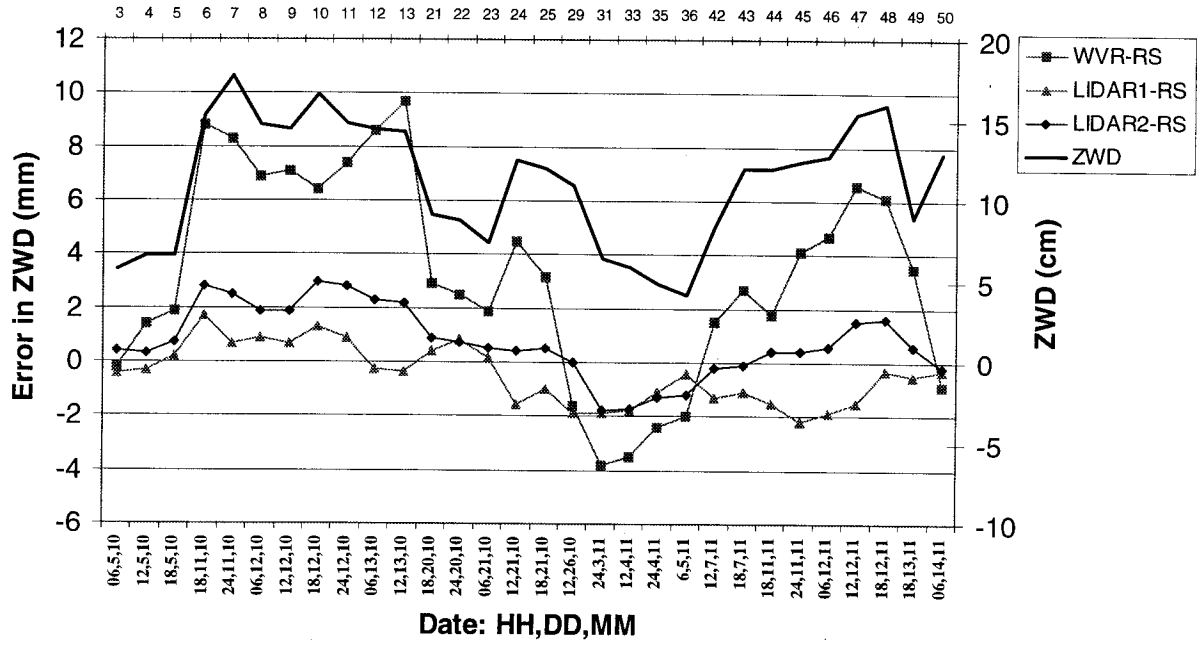

Fig. 1. Error in ZWD estimates from different techniques based on RS soundings taken as ground truth. Upper abscissa indicates the launching number.

approaches have been followed for making measurements in these conditions. In the first one, a shorter wavelength, located in the solar blind region, < 300 nm, is used (Renaut and Capitini, 1988). This method is, however, limited to boundary layer sensing, due the strong absorption by ozone at these wavelengths. In the second one, different fields-of-view for profiling the lower and higher troposphere are used (Goldsmith et al., 1998). There, a precision of about 7 %, or 1.4 mm in wet delay, is achieved at daytime for profiles up to 3.5 km.

3 Spatially resolved versus integrated measurements

In this section we compare the biases in zenith wet delay (ZWD) estimates achieved from the different techniques described in section 2. For WVRs, the $W'(s) = W'_m$ approximation is tested, with the signal evaluated from Eq.(3) and frequencies assumed to be $\nu_1 = 23.8$ GHz and $\nu_2 = 31.5$ GHz (Elgered, 1993). The model for absorption coefficient was chosen from (Rosenkranz, 1993). The error from IRSS is not readily calculated, since it is sought that it would lie somewhere between the case for WVR and for lidars. For DIAL and Raman lidars, absolute $\rho_v(s)$ measurements are assumed, and two conversion strategies to ZWD are analyzed: either a mean temperature T_m or a temperature profile from a reference radiosounding. These strategies will be referred to as Lidar1 and Lidar2, respectively.

For the evaluation of retrieval errors, we have used the radiosonde database from the Pyrénées Experiment (PYREX, 1990). Radiosonde profiles were used for evaluating the measured signals from the different techniques, and actual ZWD is evaluated from Eq.(1). Calibration errors and random errors are not considered here. This is thus rather a test for the ultimate accuracy in wet path delay achievable with these techniques.

Fig. 1 shows the errors in ZWD estimates from the different techniques along with actual ZWD, as a function of the date of the radiosounding (RS). The reference profile used for the calculation of W'_m, T_m, and $T(s)$ for the different strategies, is from 4 October 1990, 18H, for which ZWD was ~4 cm. This is a rather arbitrary choice. Results from other reference profiles gave similar statistical results, though different from day to day.

It is seen in Fig. 1 that errors of up to 1 cm in ZWD appear in WVR retrievals, with an average error of 3.3 mm and a RMS error of 3.8 mm. These results are consistent with previous studies (Elgered, 1993). The performance of both lidar retrieval strategies is much better than with WVR. Lidar1, is the best, with average and RMS errors of -0.5 and 1.1 mm, respectively, while Lidar2 has average and RMS errors of 0.75 and 1.3 mm, respectively. Virtually, these errors would vanish with a Raman lidar when $T(s)$ is computed from retrieved total density profiles, constrained by surface pressure.

Let us now focus on errors in ZWD from WVR estimates. It is first to notice that the errors are strongly correlated with ZWD. This actually reflects the effect of changes in temperature and humidity profiles. Fig. 2 shows five different cases. RS #3, was near in time with the reference profile, RS #1. Water vapor (WV) content did only slightly change, namely with a peak arising at 4 km altitude. However, this vertical inhomogeneity did quite not affect the ZWD estimate, mainly because the temperature

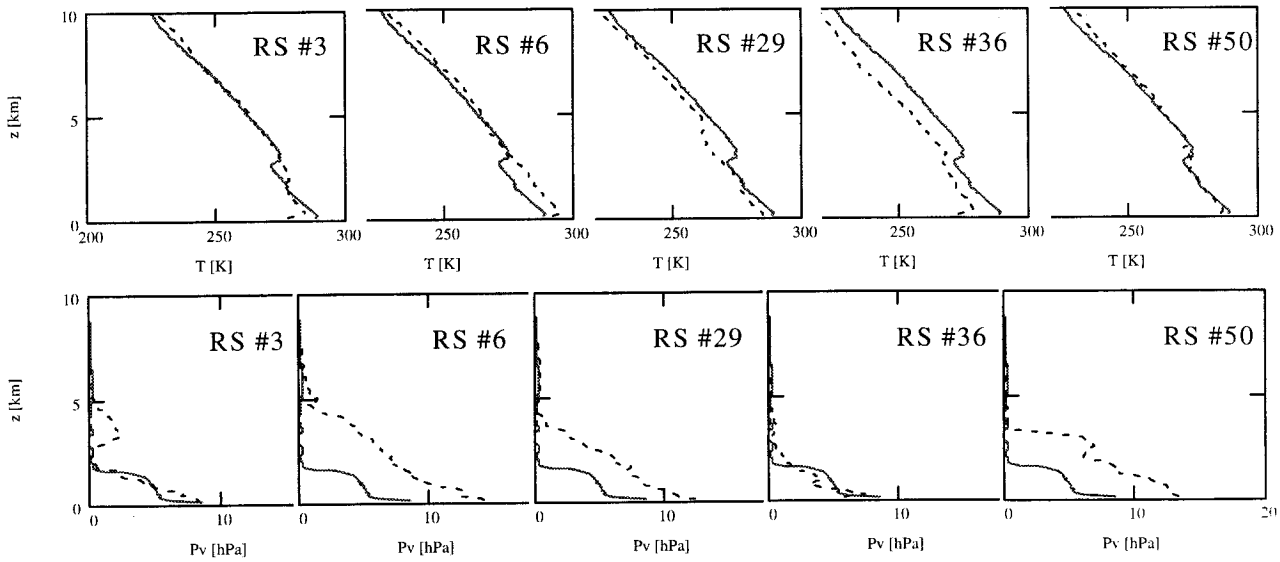

Fig. 2. Evolution of temperature (upper) and partial pressure of water vapor (lower) profiles, for launchings 3, 6, 29, 36 and 50, respectively, from left to right, in dashed lines, compared to the reference profile, from 4 October 1990, 18H, in solid line.

profile did practically not change. RS #6 shows a significant change in the temperature profile, especially, the inversion at 3 km disappeared, and in WV, which did strongly increase. The conjunction of both changes results in a bias near 9 mm in retrieved ZWD. In RS #29, the WV profile is quite similar to that of RS #6. However, the estimated ZWD is more than 1 cm smaller than the preceding. This is mainly explained by the temperature profile which is now below the reference profile and is marked by an inversion at 5 km. RS #36 also illustrates the effect of a change in temperature profile, while the WV profile is very similar to that of RS #1. RS #50 shows again that for similar temperature profiles, a strong change in WV content might almost not affect the ZWD retrieval error.

4 Discussion

It has been shown that changes in temperature profiles are an important limiting factor for ZWD retrievals by WVRs. Errors of up to 1 cm have been seen, which were roughly proportional to the total water vapor content. Though the retrieval constant W'_m can be parameterized by surface temperature, strong temperature inversions are common near the ground (see Fig. 2), which might limit the improvement with such a parameterization.

Similarly, integrated water vapor measurements retrieved by DIAL and Raman lidars can produce errors of 2-3 mm in ZWD. This accuracy is, however, better than with WVRs in similar conditions. Such an accuracy should be readily achievable, and might be sufficient for most applications. However, for applications requiring a higher accuracy, profiles of $\rho_v(s)$ and $T(s)$ are required to ensure that the effect of atmospheric inhomogeneities on path delay is properly accounted for. Therefore, Raman lidar has the highest potential, since this technique should be capable of retrieving profiles of both water vapor and dry gases concentrations. (Temperature profiles can be derived from the latter). However, for an absolute path delay correction, absolute concentration measurements are required with an accuracy better than 1 %. An independent calibration of the Raman lidar is thus necessary, which might be achieved following the approach proposed by Sherlock et al., 1999. However, we intend to study an alternative approach, consisting in calibrating the lidar with the GPS data themselves, in a similar manner as ZWD is estimated in standard GPS data analysis.

Another important advantage of Raman lidar is its capability of providing an external correction for the hydrostatic path delay. This might reduce the residual errors due to horizontal pressure and temperature gradients not properly accounted for by classical mapping functions (MacMillan and Ma, 1998).

Assuming calibrated measurements are available, retrievals of water vapor and dry gases density profiles will be still limited by several error sources, such as photon noise, due to signal and background. However, background noise can be avoided, if one restricts the lidar to night-time use only. The effect of signal induced photon noise would then result in a negligible path delay uncertainty of ~0.1 mm, based of the specifications of the CART Raman lidar (Goldsmith et al., 1998), i.e., λ_0 = 355 nm, 400 mJ/pulse, 61-cm telescope, k_{WV} = 0.06, and integrating 1800 profiles (1-min average). Thermal noise and other electronic noises, depending mainly on the detector technology and counting circuitry might be slightly more limiting, producing errors of up to ~1 mm in path delay.

The uncertainty in path delay estimates, due to these noise sources, depends on the averaging time. However, atmospheric variability might set a lower limit to the

accuracy due to turbulent fluctuations (Stull, 1988). This aspect should be carefully studied, for the optimization of the lidar performance. In addition, spatial inhomogeneities of the size of the boundary layer should be properly sensed to avoid biases (Bock, et al., 2000). Therefore, averaging time as well as the duration of the observing cycle (the lidar being assumed to point sequentially to the GPS satellites), should be properly adjusted. For comparison, pointed WVRs have proven very effective when using 30 sec–1 min observing durations and 8–15 min cycle periods for 5–8 satellites. Similar operational schemes might be achievable with a portable Raman lidar.

The final problem that should be addressed with Raman lidars is with Mie scattering from aerosols. We have evaluated that a typical 5 % bias in the aerosol extinction coefficient (Goldsmith et al., 1998) would produce an error in path delay of about 8 mm. A possibility to improve the aerosol calibration might be the use of the instrument as a passive sun or moon photometer. Infrared and visible photometers are actually capable of retrieving aerosol extinction within 2 %, which might still be further improved.

On an operational point of view, Raman lidars are much less weather proof than WVRs. While the latter are mainly limited by precipitation, lidars are additionally limited by fog and can retrieve profiles only up to cloud bases. Moreover, in the present context they are intended to operate only at night. They would thus not be fitted to replace WVRs, but rather to complement them, in the case where a high accuracy is required in specific geodetic campaigns, such as permanent GPS network calibration and national leveling network surveying, and also for atmospheric boundary layer studies.

Acknowledgments. Data from the Pyrénées Experiment (PYREX) database were used. PYREX was funded by Météo-France, Instituto Nacional de Meteorologia (INM), Centre National de la Recherche Scientifique (CNRS) and the PATOM, Electricité de France (EDF), Centre National d'Etude Spatiales (CNES), Deutche Forschungsansalt fur Luft und Raumfahrt (DLR), and Région Midi-Pyrénées, which are acknowledged.

References

Alber, C., R. Ware, C. Rocken, and F. Solheim, GPS surveying with 1 mm precision using corrections for atmospheric slant path delay, Geophys. Res. Lett., 24, 1859-1862, 1997.

Bock, O., Tarniewicz, J., Thom, C., and Pelon, J., Effect of small-scale atmospheric inhomogeneity on positioning accuracy with GPS, submitted to Geophys. Res. Lett., 2000.

Dodson, A. H., P. J. Shardlow, L. C. M. Hubbard, G. Elgered and P. O. J. Jarlemark, Wet tropospheric effects on precise relative GPS height determination, J. Geod., 70, 188-202, 1996

Elgered, G., Tropospheric radio path delay from ground-based microwave radiometry in Atmospheric remote sensing by microwave radiometry, chap. 5, M.A. Janssen (ed), Wiley, New-York, 1993.

England, M., Ferrare, R., Melfi, S.H., Whiteman, D., and Clark, T., Atmospheric water vapor measurements: Comparison of microwave radiometry and lidar, J. Geophys. Res., 97, D1, 899–916, 1992.

Glaus, R., Bürki, B., and Kahle, H.G., Recent results of water vapor radiometry in assessing vertical lithospheric movements by using space geodetic radiowave techniques, J. Geodynamics, 20, 31-39, 1995

Goldsmith, J.E.M., F. Blair, E. Bisson, and D.D. Turner, Turn-key Raman lidar for profiling atmospheric water vapor, clouds, and aerosols, Appl. Opt., 37, 4979–4990, 1998.

Ichikawa, R., et al., Estimations of atmospheric excess path delay based on three-dimensional, numerical prediction model data, J. Geod. Soc. Japan, 41, 379-408, 1995.

Johansson, J.M., T.R. Emardson, P.O.J. Jarlemark, L.P. Gradinarsky, and G. Elgered, The atmospheric influence on the results from the Swedish GPS network, Phys. Chem. Earth, 23, 107–112, 1998.

MacMillan, D.S., and C., Ma, Using meteorological data assimilation models in computing tropospheric delays at microwave frequencies, Phys. Chem. Earth, 23, 97-102, 1998.

Niell, A., Global mapping functions for the atmosphere delay at radio wavelengths, J. Geoph. Res., 101, 3227-3246, 1996.

Reagan, J.A., K.J. Thome, and B.M. Herman, A simple instrument and technique for measuring columnar water vapor via near-IR differential solar transmission measurements, IEEE Trans. Geosci. Remote Sensing, 30, 825–831, 1992.

Renaut, D., Capitini, R., Boundary-layer water vapor probing with a solar-blind Raman lidar: validations, meteorological observations and prospects, J. Atmos. Ocean Tech., Vol. 5, p. 585-601, Oct. 1988.

Rocken, C., Johnson, J.M., Neilan, R.E., Cerezo, M., Jordan, J.R., Falls, M.J., Nelson, L.D., Ware, R.H., and Hayes, M., The measurement of atmospheric water vapor: radiometer comparison and spatial variations, IEEE Trans. Geosci. Remote Sensing, 29, 3–8, 1991.

Rosenkranz, P.W., Absorption of microwaves by atmospheric gases, in Atmospheric remote sensing by microwave radiometry, chap. 2, M.A. Janssen (ed), Wiley, New-York, 1993.

Salby, M.L., Fundamentals of atmospheric physics, (Academic Press, New York, 1996).

Santerre, R., Impact of GPS satellite sky distribution, Manuscr. Geod. 16, 28–53, 1991.

Sierk, B., B. Bürki, H. Becker, S. Florek, R. Neubert, L. Kruse, and H. Kahle, Tropospheric water vapor derived from solar spectrometer, radiometer, and GPS measurements, J. Geophys. Res., 102, B10, 22,411–22,424, 1997.

Sherlock, V., A. Hauchecorne, J.Lenoble, "Methodology for the independant calibration of Raman backscatter water-vapor lidar system," Appl. Opt., Vol. 38, No. 27, 20 Sept. 1999.

Stull, R.B., An Introduction to Boundary Layer Meteorology (Atmospheric Sciences Library, Kluwer Academic, Dordrecht, The Netherlands 1988).

Tralli, D.M., and Lichten, S.M., Stochastic estimation of tropospheric path delays in Global Positioning System geodetic measurements, Bull. Geod., 64, 127–159, 1990.

Ware, R., C. Rocken, F. Solheim, T. Van Hove, C. Alber, and J. Johnson, Pointed water vapor radiometer corrections for accurate Global Positioning System surveying, Geophys. Res. Lett., 20, 2635-2638, 1993.

Westwater, E.R., Falls, M.J., and Popa Fotina, I.A., Ground-based microwave radiometric observations of precipitable water vapor: A comparison with ground truth from two radiosonde observing systems, J. Atmos. Oceanic Technol., 6, 724-730, 1989.

Whiteman , D., S.H. Melfi, R. Ferrare "Raman lidar system for measurement of water vapor and aerosols in the Earth's atmosphere," Appl. Opt., Vol. 31, pp 3068-3082, 1992.

Wu, S.C., Optimum frequencies of a passive microwave radiometer for tropospheric path length correction, IEEE Trans. Antennas Propagat., AP27, 233-239, 1979.

Wulfmeyer, W., Bösenberg, J., Ground-based differential absorption lidar for water-vapor profiling: assessment of accuracy, resolution, and meteorological applications, Appl. Opt., 37, 3825–2844, 1998.